Macromolecules

ARTICLE

pubs.acs.org/Macromolecules

Synthesis and Characterization of Solution-Processable Ladderized n-Type Naphthalene Bisimide Copolymers for OFET Applications

Matthew M. Durban,[†] Peter D. Kazarinoff,[‡] Yukari Segawa,[‡,§] and Christine K. Luscombe*[,‡]

[†]Department of Chemistry, University of Washington, Seattle, Washington 98195-1750, United States

[‡]Department of Material Science and Engineering, University of Washington, Seattle, Washington 98195-2120, United States , and

[§]Department of Organic and Polymeric Materials, Graduate School of Engineering, Tokyo Institute of Technology, 2-12-1-H120, O-okayama, Meguro-ku, Tokyo, 152-8552, Japan

Supporting Information

ABSTRACT: Solution-processable n-type ladder-based polymers are highly desirable due to their potential capability to form strong $\pi-\pi$ interactions. A series of 5 highly soluble naphthalene diimide (NDI) polymers are presented, differing in the degree to which they are able to form imine-bridged ladder polymer structures. Average electron mobilities as high as 0.0026 $cm^2 V^{-1} s^{-1}$, which show an electron-mobility improvement of 4 orders of magnitude following ladderization, and on/off current ratios on the order of 10^4 are reported for the novel material **PNDI-2BocL**, an alkyl-substituted poly(benzoquinolinophenanthrolinedione). The structure−property relationship of the aforementioned series of copolymers is presented and discussed as it pertains to organic field-effect transistor (OFET) performance.

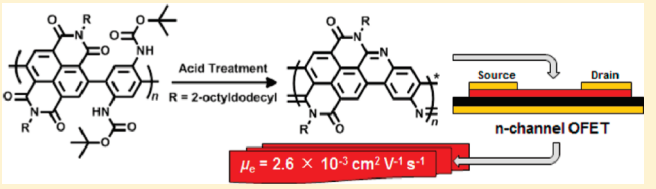

INTRODUCTION

Gradual development within the field of organic electronics has resulted in a progressive enrichment of the variety of novel materials that are available for use in a wide range of applications. Electron-transporting n-type materials are slowly beginning to gain ground with regard to their representation within the field compared to their corresponding hole-transport p-type analogues. n-Type materials have typically been hindered by issues associated with material solubility,[1,2] applicable processability, and as pertaining to photovoltaic applications, limited light absorption relative to the solar spectrum.[3] However, a variety of solution processable n-type materials have recently been synthesized and reported including; fullerenes,[4−9] acenes,[10−16] siloles,[17−19] azoles,[20] perylene,[21−28] and naphthalene diimides.[29−35] Of these materials, naphthalene diimide (NDI) copolymers[36−43] have shown exceptional promise in low-cost optoelectronic applications due to their relatively high electron mobilities,[42] solution-processability,[40,42] air-stability,[41] good light absorption characteristics,[43] and ambipolar capabilities.[44,45]

The high structural-planarity and regularity of π-conjugated ladder polymer materials can allow for desirable intermolecular $\pi-\pi$ stacking interactions as a result of improved π-electron delocalization.[46−61] Such an example has been demonstrated with the ladder material poly(benzobisimidazobenzophenanthroline) (BBL) which has shown high organic field-effect transistor (OFET) electron mobilities amid possessing poor solubility in conventional organic solvents due to its exceptional long-range packing order and crystallinity.[62] Meanwhile, there remains a limited amount of available information pertaining to soluble heteroaromatic ladder polymer materials.[63] Novel solution-processable ladder polymers are thus desirable in addressing a goal toward improving organic electronic device performance.

Additional insight into the structure−property relationships associated with naphthalene-diimide copolymers is presented through the synthesis and characterization of a series of solution processable naphthalene diimide-based, di-*tert*-butyl dicarbonate (Boc) substituted benzene copolymers (**PNDI-0Boc** [an alkyl-substituted poly(benzophenanthrolinetetraone)], **PNDI-1Boc** [an alkyl-substituted poly(benzophenanthrolinetetraone-phenylcarbamate)], and **PNDI-2Boc** [an alkyl-substituted poly(benzophenanthrolinetetraone-phenyldicarbamate)], see Scheme 1 for the monomers and Scheme 2 for the polymers) which are capable of undergoing a solution-based intramolecular cyclization process[64−67] in yielding soluble n-type ladder polymer materials (**PNDI-1BocL**, which is an alkyl-substituted poly(benzoquinolinophenanthrolinetrione) and **PNDI-2BocL**, an alkyl-substituted poly(benzoquinolinophenanthrolinedione), see Scheme 2). To our knowledge, these are the first n-type ladder polymers, which are soluble in common organic solvents, to be reported. Recently, a series of soluble high-performance naphthalene diimide core donor−acceptor based polymers (using the same naphthalene diimide core as the materials presented in this report) containing a varying number of thiophene subunits within the polymer backbone was reported by our

Received: March 2, 2011
Revised: May 21, 2011
Published: June 03, 2011

Scheme 1. Characteristic Stannylated-BOC-Monomer Synthesis[a]

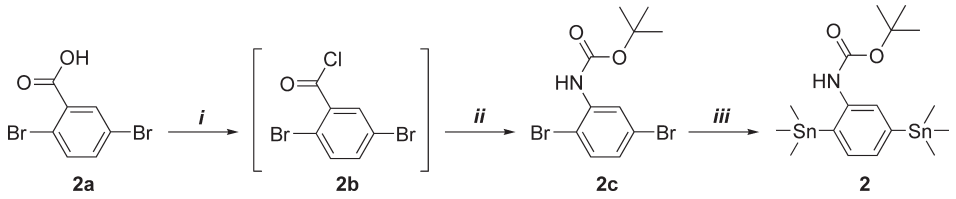

[a] Key: *i*, oxalyl chloride, cat. DMF; *ii*, NaN_3, $^tBuNH_4Br$, ^tBuOH; *iii*, MeLi, ^tBuLi, trimethyltin chloride.

Scheme 2. NDI Polymer Synthesis and Ladderization[a]

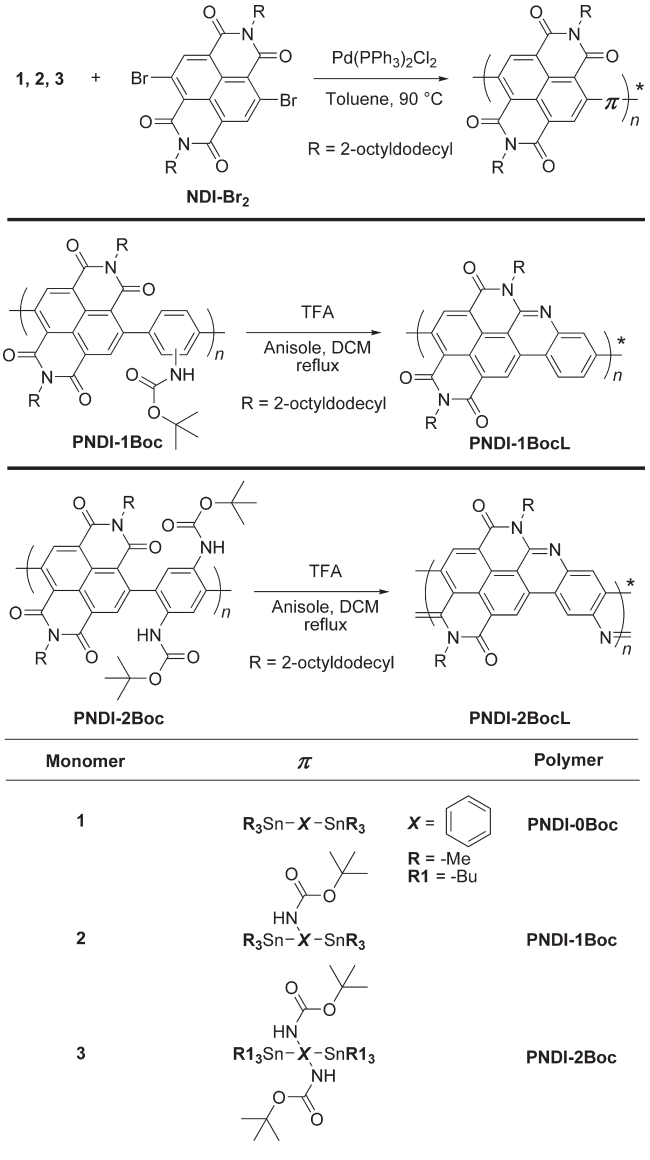

Monomer	π	Polymer
1	$R_3Sn-X-SnR_3$	PNDI-0Boc
2	$R_3Sn-X-SnR_3$	PNDI-1Boc
3	$R1_3Sn-X-SnR1_3$	PNDI-2Boc

[a] The asterisk denotes that Stille coupling reaction NDI-polymers were end-capped with phenyl groups using 1-bromobenzene.

group.[43] OFET electron mobilities as high as 0.076 $cm^2\ V^{-1}\ s^{-1}$ were achieved using the novel material PNDI-3Th (an alkyl-substituted poly[terthiophenebenzophenanthrolinetetraone]) and provided incentive into developing a soluble NDI-based ladder polymer. A soluble-precursor polymer (**PNDI-1Boc** and **PNDI-2Boc**) route was initially investigated whereby the precursor thin films were thermally treated to remove the Boc groups and promote cyclization. However, naphthalene diimide's branched octyl-dodecyl solubilizing chains proved to be sufficiently capable of bestowing solubility upon the final ladderized polymer products (**PNDI-1BocL** and **PNDI-2BocL**). Therefore, solution based cyclization routes were used to obtain the final ladderized structures.

EXPERIMENTAL SECTION

Instrumentation and Materials. ^1H and ^{13}C NMR spectra were obtained using a Bruker AV-300 or AV-500 spectrometer. Polymer molecular weights were obtained using a Waters-1515 gel permeation chromatograph (GPC) coupled with UV and RI detectors. Polystyrene GPC standards in THF were used as a reference. Cyclic voltammetry for all polymers was obtained under nitrogen using a BAS CV-50 W voltammetric analyzer with 0.1 M tetra-*n*-butylammonium hexafluorophosphate in anhydrous acetonitrile as supporting electrolyte. A platinum wire working and counter electrode as well as an $Ag/AgNO_3$ reference electrode was used and ferrocene (Fc/Fc^+) was designated as an internal standard for all measurements. The scan rate was 50 mV/s. The reference energy level used for ferrocene as compared to vacuum was 4.8 eV. A HP4145B semiconductor parameter analyzer controlled by locally written LabView codes through a GPIB interface was used for OFET device characterization. All device fabrication and electrical characterization were performed in a nitrogen atmosphere. Samples for UV/vis, FTIR, and X-ray diffraction analysis were cleaned prior to use. Absorption spectra were obtained using a Varian Cary 5000 UV–vis–NIR spectrophotometer. FTIR spectra were obtained using a Bruker Vector 33 Fourier transform infrared spectrophotometer equipped to analyze NaCl sample plates. Mass spectrometer data (HR/LR) was obtained using a JEOL HX-110 mass spectrometer and a Bruker Esquire LC-Ion Trap mass spectrometer. Density functional theory (DFT) calculations were performed using the Gaussian 03 software package using the B3LYP calculation method and 6-31G basis set.[68−70] Geometry optimization followed by frequency calculation was performed to obtain the lowest energy conformations. All reagents (including **2a**) used for synthesis were obtained from Sigma-Aldrich and were used as-is without further purification with the exception of the catalyst, Pd-$(PPh_3)_2Cl_2$, which was obtained from Strem Chemicals.

Synthetic Procedures. The monomers used to synthesize the NDI-polymers were synthesized using standard literature procedures—specifically, NDI–Br_2,[40,42,71,72] and the stannylated phenyl monomers; **1**[73] and **3**.[74]

Synthesis of ***2c***. To a 100 mL air-free Schlenk flask, 2,5-dibromobenzoic acid (**2a**) (2.5 g, 8.9 mmol) was added to 30 mL of toluene followed by oxalyl chloride (1.7 g, 13.4 mmol) and a catalytic amount of DMF (1 drop). The solution was heated at reflux for 2 h. The gold-colored clear reaction solution was cooled to room temperature to provide a yellow residue (**2b**) after the solvent was removed under reduced pressure, which was not isolated. The residue was dissolved in dry dichloromethane (14 mL) and added dropwise to a solution of

Table 1. Polymer Properties and Yields

	yield (%)	M_n (kDa) [PDI][a]	soln λ_{max}[b] abs (nm)	film λ_{max}[c] abs (nm)	E_g^{opt}[d] (eV)	$E_{1/2red}$[e] (V)	LUMO[f] (eV)	HOMO[g] (eV)
PNDI-0Boc	87	8.8 [2.5]	453	471	2.31	−0.96	−3.79	−6.10
PNDI-1Boc	74	4.0 [1.8]	380	384	2.19	−0.90	−3.83	−6.02
PNDI-2Boc	76	7.2 [1.6]	381	382	1.94	−0.84	−3.90	−5.84
PNDI-1BocL	74	4.3 [1.9]	467	476	2.37	−1.20	−3.54	−5.90
PNDI-2BocL	93	14 [1.8]	578	576	1.96	−1.18	−3.54	−5.49

[a] Number-average molecular weight and polydispersity (SEC vs polystyrene standards in THF). [b] Solution absorption spectra ($\sim 5 \times 10^{-6}$ M $CHCl_3$). [c] Thin film absorption spectra from spin-cast $CHCl_3$ solutions. [d] Optical energy gap estimated from the absorption-edge or onset of organic thin films. [e] CV measurements of thin films vs Fc/Fc^+. [f] Estimated from LUMO = −(normalized Fc/Fc^+) − $E_{1/2red}$. [g] Estimated from HOMO = LUMO − E_g^{opt}.

saturated (6.4 M) sodium azide (7 mL), ^{t}BuNH$_4$Br (4.1 mg), and dichloromethane (3.5 mL) at −5 °C over 1.5 h. The biphasic mixture was stirred for 10 min after the addition was complete. The organic phase was separated and the aqueous phase was extracted with cold dichloromethane (2 × 20 mL). The organic phases were combined and washed with cold water (2 × 30 mL). The solution was then dried over $MgSO_4$ at 0 °C and filtered over a mixture of Celite and $MgSO_4$. The filtrate was subsequently dried over CaH_2 at 0 °C for 40 min. The mixture was filtered again through a pad of Celite and $MgSO_4$. The light yellow filtrate was added to ^{t}BuOH (15 mL) and heated at reflux overnight. The cloudy-white solution was cooled to room temperature and the solvent removed under reduced pressure to provide an off-white solid. The residue was purified via flash chromatography using a mixture of ethyl acetate and hexane (1:4) as eluent. **2c** was isolated as a white solid (2.4 g, 77%). ^{1}H (300 MHz, $CDCl_3$): δ 8.32 (d, 1H), 7.26 (d, 1H), 6.94 (dd, 1H), 6.92 (s, 1H), 1.46 (s, 9H). ^{13}C (75 MHz, $CDCl_3$): δ 151.9, 137.4, 133.1, 126.6, 122.5, 122.0, 110.5, 81.6, 28.2 (3). HRMS-FAB$^+$ (m/z): calcd for $C_{11}H_{13}O_2NBr_2$, 350.92947; found, 350.92859; m/z 351 (14%), 296 (39%), 251 (16%), 165 (8%), 154 (100%), 107 (32%).

Synthesis of ***2***. A 50 mL air-free Schlenk flask was charged with **2c** (1.1 g, 3.1 mmol) in diethyl ether (20 mL) at −78 °C. 1.6 M MeLi (2.05 mL, 3.3 mmol) was added to the solution dropwise and allowed to stir for 10 min at −78 °C. The solution was allowed to warm to 0 °C. The yellow solution was slowly transferred via cannula to a 100 mL air-free Schlenk flask containing 1.7 M ^{t}BuLi (6.08 mL, 10.3 mmol) in diethyl ether (7 mL) at −78 °C. The mixture was stirred for 4 h at −78 °C before allowing the reaction to slowly warm to 0 °C. The dark orange slurry was recooled to −78 °C before adding 1 M trimethyltin chloride (8.33 mL, 8.33 mmol). The light clear orange solution was allowed to warm to 0 °C before quenching with water (20 mL). The organics were separated and the aqueous phase was extracted with diethyl ether (2 × 20 mL). The organics were combined and washed with water (2 × 30 mL) and brine (30 mL). The isolated organics were dried over Na_2SO_4, filtered, and the solvent removed under reduced pressure to produce a red-orange oil. The residue was purified via flash chromatography by eluting through basic silica (treated with 9:1 hexane: triethylamine) using hexane as eluent. **2** was isolated as a white crystalline solid (0.31 g, 19%). ^{1}H (300 MHz, $CDCl_3$): 7.56 (s, 1H), 7.39 (d, 1H), 7.25 (d, 1H), 6.24 (s, 1H), 1.50 (s, 9H), 0.32 (s, 9H), 0.28 (s, 9H). ^{13}C (75 MHz, $CDCl_3$): δ 153.93, 143.68, 142.82, 136.42, 136.03, 132.23, 130.53, 80.28, 28.44 (3), −8.55 (3), −9.49 (3). MS/EI: m/z 540 (Na^+), 504 (17%), 448 (100%), 400 (10%), 286 (15%), 165 (46%), 135 (10%).

General Synthesis for PNDI-xBoc. To an air-free Schlenk flask, $Pd(PPh_3)_2Cl_2$ (0.005 mmol), NDI−Br_2 (0.10 mmol), and **1**,[73] **2**, or **3**[74] (0.10 mmol) were added within a dry glovebox and dissolved with toluene (5 mL). The capped and sealed vessel was heated at 90 °C for 4 days prior to injecting bromobenzene (0.2 mL) and stirring for 12 h. The reaction was cooled to ambient and KF (1 g) in water (2 mL) was injected and stirred for 2 h. The solution was extracted with chloroform (2 × 60 mL). The combined organics were washed with water (2 × 50 mL) and dried over Na_2SO_4. The solution was concentrated by vacuum and precipitated into methanol. The precipitated polymer was subjected to a Soxhlet extraction with acetone and methanol for 48 h to remove low-molecular weight polymer fragments. The polymer was redissolved in chloroform, precipitated into methanol, and dried under reduced pressure. See Table 1 for further polymer data. **PNDI-0Boc**: orange solid (87%). ^{1}H (300 MHz, $CDCl_3$): 8.89 (br, 2H), 7.58 (br, 4H), 4.11 (br, 4H), 2.01 (m, 2H), 1.03−1.49 (m, 64H), 0.84 (m, 12H). ^{13}C (300 MHz, $CDCl_3$): 163−162, 147, 140, 136, 129−128, 128−125, 124−123, 45, 37−36, 32, 31, 30−29, 26, 23−22, 14. **PNDI-1Boc**: red solid (74%). ^{1}H (500 MHz, $CDCl_3$): 8.90 (br, 2H), 8.26 (br, 1H), 7.92−7.51 (br, 1H), 7.30 (br, 1H), 6.12 (br, 1H), 4.15 (br, 4H), 2.04 (m, 2H), 0.97−1.73 (m, 73H), 0.86 (m, 12H). ^{13}C (125 MHz, $CDCl_3$): 163−162, 153−152, 147, 144, 141, 137−134, 129−123, 81−80, 45, 37−36, 32−31, 31−29, 29−28, 27−26, 23−22, 14. **PNDI-2Boc**: brown-red solid (76%). ^{1}H (500 MHz, $CDCl_3$): 8.91 (br, 2H), 7.99 (br, 2H), 6.03 (br, 2H), 4.16 (br, 4H), 2.03 (m, 2H), 0.99−1.61 (m, 82H), 0.85 (m, 12H). ^{13}C (125 MHz, $CDCl_3$): 164−160, 154−152, 144−143, 141, 139−136, 134−130, 129−123, 122−119, 81−80, 45, 37−36, 32−31, 31−29, 29−27, 27−26, 23−22, 14.

General Ladderization Treatment Generating ***PNDI-xBocL***. Literature procedures were adapted to form the ladder polymers.[74] To a single-neck round-bottom flask, **PNDI-*x*Boc** (0.1 mmol) was dissolved in dichloromethane (5−10 mL). Trifluoroacetic acid (3−4 mL) and anisole (0.5 mL) were added and the mixture was heated at reflux overnight. The reaction solution was subsequently cooled to room temperature and the solution was carefully and slowly added to a mixed solvent of triethylamine (10 mL) and acetone (100 mL). The precipitate was collected by filtration and then dissolved in triethylamine (5 mL). The solution was heated in a screw-cap vial at 80 °C overnight. The solution was then cooled to room temperature, precipitated in acetone, and filtered. The solids were washed with acetone and dried to yield the final ladderized polymer product. **PNDI-1BocL**: red solid (74%). ^{1}H (500 MHz, $CDCl_3$): 9.74−10.50 (br, 2H), 7.83−9.53 (br, 3H), 3.79−4.52 (br, 4H), 1.88−2.52 (m, 2H), 0.95−1.79 (m, 64H), 0.84 (m, 12H). ^{13}C (125 MHz, $CDCl_3$): 165−160, 150−140, 138−134, 130−120, 110, 45, 37−36, 32−31, 31−29, 27−26, 23−22, 14. **PNDI-2BocL**: violet-black solid (93%). ^{1}H (500 MHz, $CDCl_3$): 9.63−10.50 (br, 1H), 9.24 (br, 2H), 7.04−8.76 (br, 1H), 5.23 (br, 4H), 2.37 (m, 2H), 1.04−2.25 (m, 64H), 0.87 (m, 12H). ^{13}C (125 MHz, $CDCl_3$): 165−158, 151−146, 145−137, 135−117, 115−106, 45, 37−35, 32−31, 31−29, 29−27, 27−26, 23−22, 14.

OFET Device Fabrication. Thin film transistors were fabricated as typical top-contact bottom-gate devices on silicon substrates. Heavily doped p-type silicon ⟨100⟩ substrates from Montco Silicon Technologies Inc. with a 300 nm (±5 nm) thermal oxide layer acted as common gate, dielectric layer, and substrate. The substrates were cleaned by sequential ultrasonication in acetone, methanol, and isopropyl alcohol for 10 min followed by an air plasma treatment. The optimized conditions used for obtaining the electron mobility measurements are

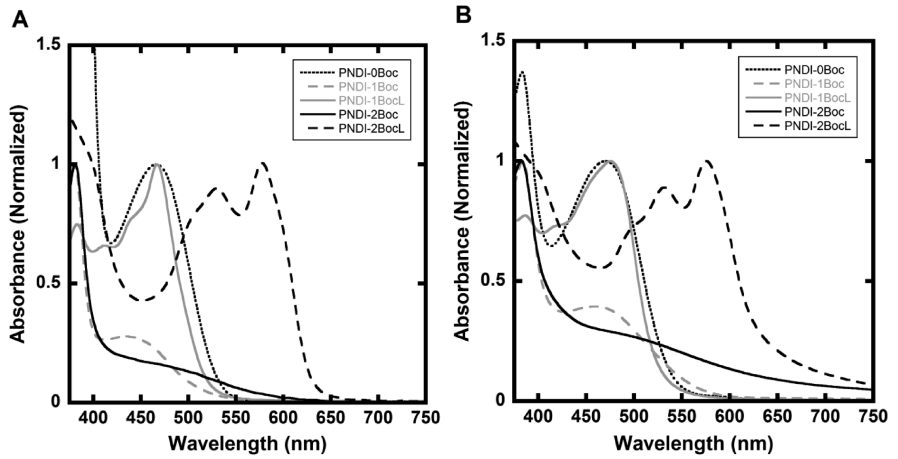

Figure 1. (A) Solution UV/vis absorption spectra ($\sim 5 \times 10^{-6}$ M $CHCl_3$) and (B) thin-film UV/vis absorption spectra.

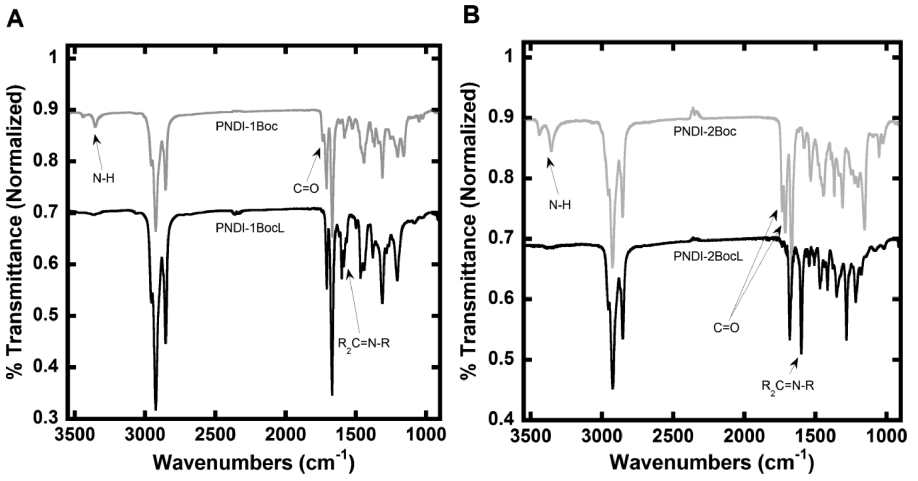

Figure 2. (A) Spectra of **PNDI-1Boc** before and after ladderization and (B) respective spectra of **PNDI-2Boc**.

as follows: polymer thin films were deposited from a filtered 5 mg/mL chlorobenzene solution by spin-coating at 1000 rpm for 60 s (octadecyltrichlorosilane (OTS) treated substrates were also used, but yielded poor performance compared to devices fabricated on bare oxide layer substrates). The devices were dried on a temperature-controlled hot-plate at 150 °C for 10 min under nitrogen atmosphere. Interdigitated source and drain electrodes (W = 9000 μm, L = 90 μm) made of gold (50 nm thick) were deposited through shadow masks on top of the polymer active layer by thermo evaporation at 1.0 Å/s by a resistively heated Mo boat under high vacuum (5.0×10^{-7} Torr). At least four devices were fabricated to obtain average electron mobilities.

RESULTS AND DISCUSSION

The highly electron-deficient naphthalene diimide acceptor unit with branched-alkane, octyldodecyl-, solubilizing groups was copolymerized with *p*-bis(trimethylstannyl)benzene (**1**),[73] *N*-(*tert*-butoxycarbonyl)-1-amino-2,5-bis(trimethylstannyl)benzene (**2**), and *N*,*N*′-bis(*tert*-butoxycarbonyl)-1,4-diamino-2,5-bis(tri-*n*-butylstannyl)benzene (**3**),[74] using Stille conditions and $Pd(PPh_3)_2Cl_2$ as catalyst (see Scheme 2). The mono- and di-Boc-functionalized stannyl comonomers were chosen due to their acid-sensitivity in yielding free amine groups which are capable of reacting with adjacent carbonyl (imide) groups in forming intramolecular imine-bridged planar structures.[74] The di-Boc functionalized stannyl monomer, **3**, is capable of forming imine-bridged structures with both ends of the adjacent naphthalene diimide comonomer in generating a fully ladderized copolymer. Whereas, the monoboc functionalized stannyl monomer, **2**, is capable of only reacting with one of the two adjacent naphthalene comonomers in thereby forming a copolymer with localized ladder polymer structures. The stannyl monomer with no Boc functionalities, **1**, was thus used to synthesize a polymer with no imine-bridges for comparative reference purposes. Monomer **2** was synthesized using a procedure analgous to the method referenced for **3** in which a commercially available functionalized benzoic acid compound was reactively converted to an isocyanate which spontaneously underwent a Curtius rearrangement (Scheme 1).[74] Hydrolysis by *tert*-butyl alcohol yields the final target as a Boc-protected amine, **2c**. Stannylation was performed by deprotonation of the Boc−amine by MeLi followed by bromine−lithium exchange using ^{t}BuLi and quenching with trimethyltin chloride.

Solutions of the dissolved Boc-containing copolymers, **PNDI-1Boc** and **PNDI-2Boc**, were treated with trifluoroacetic acid at elevated temperatures to cleave the electronically insulating Boc groups and form intramolecular imine-bridges to generate

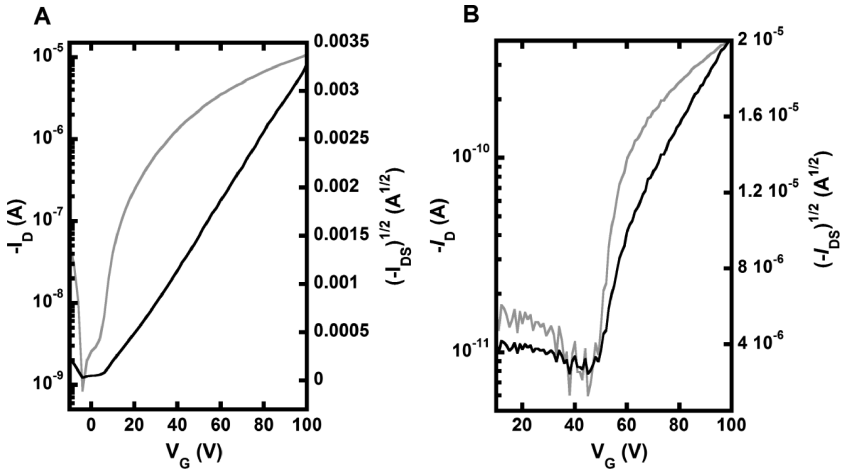

Figure 3. (A) Transfer curve of **PNDI-2BocL** and (B) **PNDI-2Boc** at a constant source-drain voltage of +100 V plotted with the square root of current as a function of gate voltage.

Table 2. Electrical Characterization of NDI Co-Polymers

	μ_e[a] ($cm^2\ V^{-1}\ s^{-1}$)	$I_{on/off}$	V_t (V)
PNDI-0Boc	6×10^{-6} ($\pm 1 \times 10^{-6}$)	10^4	9
PNDI-1Boc	4×10^{-6} ($\pm 1 \times 10^{-6}$)	10^2	10
PNDI-2Boc	1.9×10^{-6} ($\pm 4 \times 10^{-7}$)	10^2	50
PNDI-1BocL	4×10^{-7} ($\pm 1 \times 10^{-7}$)	10^2	7
PNDI-2BocL	2.6×10^{-3} ($\pm 4 \times 10^{-4}$)	10^4	5

[a] Average value of at least four devices with standard deviation. Calculated from the $I_{ds}^{1/2}$ vs V_g plot using the equation $I_{ds} = (\mu W C_o / 2L)\cdot(V_g - V_t)^2$.

Table 3. DFT Computed PNDI Sub-Unit Dihedral (Torsion) Angles in Deg

	0Boc	1BocL	2BocL	1Th
$C_1-C_2-C_3-X_4$[a]	55.06	−61.87	0	−41.21

[a] X = C for PNDI-0Boc, PNDI-1BocL, and PNDI-2BocL, X = S for PNDI-1Th.

PNDI-1BocL and **PNDI-2BocL**. The molecular weights of all polymers synthesized were determined using size-exclusion chromatography (SEC) relative to polystyrene standards in THF and are listed in Table 1. Determination of polymer molecular weights via integrative NMR calculations was not possible since the peaks for the terminal phenyl groups overlapped with the polymer peaks. The polymer molecular weights were recognized as being overestimations of the actual polymer mass due to NDI's rigid-rod-like polymeric character and the additional rigidity incurred by ladderization.[75] Increasing the planarity of the copolymers by this means will effectively increase the hydrodynamic radius of the polymer when characterized by SEC. This phenomenon was observed in that the respective polymer molecular weights increased to a degree following ladderization. In the case of **PNDI-2Boc**, the molecular weight nearly doubled from 7.2 to 14 kDa.

Optical absorption spectra (Figure 1) were taken for all five polymer films spin coated from $CHCl_3$ onto glass revealing a marked red-shift of the absorption band for **PNDI-1Boc** and **PNDI-2Boc** when compared to the polymer absorption spectra after ladderization. The **PNDI-1Boc** spectrum reveals a shift from λ_{max} = 384 nm to λ_{max} = 476 nm for **PNDI-1BocL** as a result of this structural transformation. Likewise, a similar trend is observed for **PNDI-2Boc** with a higher magnitude shift from λ_{max} = 382 nm to λ_{max} = 576 nm for **PNDI-2BocL**. The absorption maximum similarity between **PNDI-1Boc** and **PNDI-2Boc** may be caused by the relatively bulky Boc-functional groups which inhibit the absorption of each polymer to a similar degree. **PNDI-0Boc** thus exhibits comparatively improved absorption characteristics due to its lack of any Boc functional groups. Furthermore, the absorption spectrum of **PNDI-1BocL** closely resembles that of **PNDI-0Boc** as a result of Boc-removal. The reduced conjugation length of **PNDI-1BocL** (E_g = 2.37 eV) compared to **PNDI-2BocL** (E_g = 1.96 eV) is likely due to the greater number of rotational degrees of freedom (polymer backbone twists) in **PNDI-1BocL** which allow for potential breaks in π-conjugation between individual ladderized subunits. While there is not a significant band gap difference between **PNDI-2Boc** and **PNDI-2BocL**, the large observed λ_{max} shift appears to be a result of the extended imine-bridge ladder structure functioning as an improved absorptive chromophore. Additionally, the large red-shift in the λ_{max} for the charge-transfer band (531 nm) of the UV−vis absorption spectrum of **PNDI-2BocL** shows further evidence of the existence of extensive conjugation in imine-bridged ladder polymer systems.[64]

Imine-bridge formation was further confirmed by FTIR analysis (Figure 2) before and after the ladderization reaction step. The most notable confirmation is evident in the loss of the two −N−H stretch peaks at 3360 and 3450 cm^{-1} which correspond to the loss of the Boc functionality in both the **PNDI-1BocL** and **PNDI-2BocL** spectra. Further evidence of imine-bridge formation can be seen in the loss of a -C═O stretch peak at 1740 cm^{-1} in the **PNDI-1Boc** spectrum and a loss of two corresponding peaks at 1715 and 1735 cm^{-1} in the **PNDI-2Boc** spectrum coupled with the significant gain of a single imine stretch peak at 1600 cm^{-1} for **PNDI-2BocL** and the gain of several in the same location for the **PNDI-1BocL** spectrum due to the existence of several isomeric polymer structures. The relatively low-intensity of the −C═O stretch for the BOC-group in the **PNDI-1Boc** spectrum can be attributed to the reduced abundance of the BOC-functional group compared to the

dx.doi.org/10.1021/ma2004822 |*Macromolecules* 2011, 44, 4721–4728

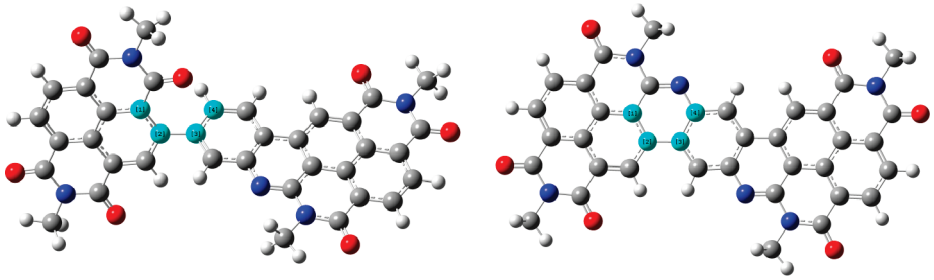

Figure 4. DFT computed reduced-geometry structures of **PNDI-1BocL** (left) and **PNDI-2BocL** (right).

PNDI-2Boc polymer material and other carbonyl-containing organic molecules.

The LUMO energy levels were calculated from the onset of the first polymer reduction peak using cyclic voltammetry. Cyclic voltammetry was carried out in a standard three-electrode electrochemical cell employed with a platinum working electrode and a $Ag/AgNO_3$ reference electrode while using ferrocene as an internal standard. The energy level referenced for ferrocene compared to vacuum was 4.8 eV.[76] As observed in our previous study of NDI−thiophene copolymers, the LUMO values for all polymers in our current study that possessed unmodified NDI cores (**PNDI-0Boc**, **PNDI-1Boc**, **PNDI-2Boc**) were found to be approximated to ∼-3.8 eV due to the intrinsic properties of NDI.[42,43,71,77] However, modification of the NDI backbone due to imine-bridge formation after ladderization was found to raise the LUMO to −3.54 eV for both **PNDI-1BocL** and **PNDI-2BocL** due to a slight reduction in electron-deficiency as a result of forming an imine-bridge in place of a more electron-withdrawing carbonyl oxygen. The HOMO values were calculated using the optical band gap (E_g^{opt}) from the calculated LUMO. The compiled data is presented in Table 1. No oxidation waves were observed for any of the five NDI polymers.

OFET devices using the five polymers were fabricated using typical top-contact, bottom-gate geometry on doped-Si/SiO_2 wafers. The active layers of the devices were spin-cast from a 5 mg/mL solution of chlorobenzene. All fabrication and testing was performed in an inert atmosphere.

Each of the five polymers showed n-type behavior at positive gate-source biases ($V_g = +100$ V). The polymers did not display ambipolar or p-type response; exhibiting low current flow, and on/off ratios below 10 when a negative gate-source bias was applied ($V_g = -100$ V). A linear fit was applied in the saturation region of the $I_{ds}^{1/2}$ vs V_G curve to calculate the saturated charge carrier mobility of each material according to the saturation current equation: $I_{ds} = (\mu WC_0/2L)(V_g - V_t)^2$.[78]

An electron mobility (μ_e) as high as 2.6×10^{-3} cm^2 V^{-1} s^{-1} was measured from OFETs yielded by **PNDI-2BocL** (Figure 3). As shown in Table 2, **PNDI-2BocL** was found to possess the highest charge carrier mobility of the series—an increase of over 3 orders of magnitude compared to the nonladderized **PNDI-2Boc** (1.9×10^{-6} cm^2 V^{-1} s^{-1}). Very little change in electron mobility was observed between **PNDI-1Boc** and its ladderized constituent **PNDI-1BocL**. **PNDI-0Boc** also performed similarly compared to the polymers **PNDI-1Boc** and **PNDI-1BocL**. As can be seen in Figure 3, although the on/off ratio of **PNDI-0Boc** was the same as the on/off ratio for **PNDI-2BocL**, both the I_{on} and I_{off} for **PNDI-0Boc** was greatly reduced compared to **PNDI-2BocL**. Complete ladderization in the case of **PNDI-2BocL** led to an increase in electron mobility, whereas the locally ladderized-subunit structure of **PNDI-1BocL** showed negligible performance gains following imine-bridge formation. Furthermore, the 5 polymers were analyzed by X-ray diffraction (XRD). However, the XRD characterization performed on the polymer series yielded no distinct peaks—indicating that the 5 NDI polymers have very little, if any, long-range ordering in the solid state. This is further supported by the lack of a significant shift between the solution and solid state UV/vis spectra of the polymer series. Varying OFET device annealing temperatures between 80 and 200 °C had little effect on the electron charge mobility which may also coincide with the lack of a phase transition in this temperature range. In addition, surface morphology of the polymer films as observed by AFM showed no distinct features, which led us to believe the morphology in the thin films was amorphous in nature. While this insight may lead one to believe that the ladder polymers were amorphously cross-linked—solid-state ladderization experiments were performed on polymer thin-films of **PNDI-2Boc** by heating and annealing the polymers to ∼250 °C. The characterized **PNDI-2BocL** films made by this process showed the same indicative FTIR and UV−vis spectra coinciding with imine-bridge formation. However, the solid-state generated ladder polymer films were completely insoluble amid exposure to all common organic solvents, exhibited entirely amorphous structures, and performed poorly in OFET devices as a result of the formed cross-linked polymer structures.

DFT calculations were conducted to determine the potential twist geometry present within **PNDI-0Boc**, **PNDI-1BocL**, and **PNDI-2BocL** as related to OFET device performance. The geometry of **PNDI-1Th**, a high-performing ($\mu_e = 3.1 \times 10^{-3}$ cm^2 V^{-1} s^{-1}) polymer analogue to PNDI-0Boc (with a thiophene replacing the benzene comonomer component) previously synthesized and reported by our lab,[43] was also calculated to determine if additional geometry-performance correlations could be made. The geometries and electronic structures of methyl-substituent analogues of all calculated polymers were analyzed with Gaussian 03 software.[70] Becke's three-parameter gradient-corrected function (B3LYP) with a polarized 6-31G basis set was used for full geometry optimization.[68,69] Methyl groups were used in approximation of the branched octyl−dodecyl alkyl chains and polymers were reduced to three monomeric subunits focused around the benzene component in order to limit calculation time. DFT computed dihedral (torsion) angles between NDI and adjacent aromatic rings (phenyl or thiophene) of the listed polymers are summarized in Table 3 while structures for **PNDI-1BocL** and **PNDI-2BocL** are shown in Figure 4. As predicted, there is a sufficiently large 55.06° out-of-plane twist of the phenyl component of **PNDI-0Boc** as well as within **PNDI-1BocL** (−61.87°) which appears to

exhibit a backbone consisting of alternating in-plane and out-of-plane subunits which would severely hinder $\pi-\pi$ stacking and device performance as seen in Table 2. Likewise, **PNDI-2BocL** which exhibited the highest OFET device performance was predicted to possess a planar polymer architecture lacking in the torsional strain seen with **PNDI-1BocL** which would aid in facilitating charge transport. The thiophene analogue, **PNDI-1Th**, possessed a calculated dihedral angle of $-41.21°$ which renders the polymer with slightly improved planarity compared to **PNDI-0Boc** and **PNDI-1BocL**. However, **PNDI-2BocL**, with a theoretically fully planar geometry shows similar performance with respect to its charge mobility by **PNDI-1Th** (3.1×10^{-3} cm^2 V^{-1} s^{-1}).[43] Further structural studies of the thin film are currently being performed to elucidate why, despite the increased planarity, **PNDI-2BocL** and **PNDI-1Th** show similar mobilities: the two polymers may orient differently with respect to the surface, which will affect OFET mobilities.

CONCLUSION

A series of high-performance NDI-based substituted-phenylene copolymers capable of forming ladderized imine-bridges following treatment with TFA have been presented. Imine-bridge formation was confirmed by FTIR, UV−vis, and CV. Average electron mobilities as high as 0.0026 cm^2 V^{-1} s^{-1} were achieved for OFETs from **PNDI-2BocL**. The charge-carrier mobility of the ladderized material, **PNDI-2BocL**, showed a 3 orders of magnitude increase compared to the linear-chain **PNDI-2Boc**. XRD and AFM results have shown the materials to be primarily amorphous; however investigation toward determining whether the polymer series stacks in a different plane in the solid-state compared to NDI-thiophene-based copolymers is currently being investigated. The relatively high electron-mobility, energy levels, and good absorption spectrum of **PNDI-2BocL** suggest the polymer's potential for use as the n-type component of various device applications. Research into further material and device optimization and the performance of organic photovoltaic (OPV) devices is the subject of future investigation.

ASSOCIATED CONTENT

Supporting Information. Figures showing cyclic voltammetry reduction curves, OFET transfer curves for all described polymers, DFT computed structures for pertinent materials, PNDI-1BocL isomeric structures, and ^1H and ^{13}C NMR spectra. This material is available free of charge via the Internet at http://pubs.acs.org.

AUTHOR INFORMATION

Corresponding Author
*E-mail: luscombe@u.washington.edu.

ACKNOWLEDGMENT

The authors would like to acknowledge the NSF (CAREER Award DMR 0747489, SOLAR Award DMR 1035196), the DOE Solar America Initiative, and the Yoshida Scholarship Foundation Initiative for financial support.

REFERENCES

(1) Hummelen, J. C.; Knight, B. W.; Lepeq, F.; Wudl, F.; Yao, J.; Wilkins, C. L. *J. Org. Chem.* **1995**, *60*, 532.
(2) Janssen, R. A. J.; Hummelen, J. C.; Wudl, F. *J. Am. Chem. Soc.* **1995**, *117*, 544.
(3) Wienk, M. M.; Kroon, J. M.; Verhees, W. J. H.; Knol, J.; Hummelen, J. C.; van Hal, P. A.; Janssen, R. A. J. *Angew. Chem., Int. Ed.* **2003**, *42*, 3371.
(4) Haddon, R. C. *J. Am. Chem. Soc.* **1996**, *118*, 3041.
(5) Bendikov, M.; Wudl, F.; Perepichka, D. F. *Chem. Rev.* **2004**, *104*, 4891.
(6) Waldauf, C.; Schilinsky, P.; Perisutti, M.; Hauch, J.; Brabec, C. J. *Adv. Mater.* **2003**, *15*, 2084.
(7) Yang, C.; Kim, J. Y.; Cho, S.; Lee, J. K.; Heeger, A. J.; Wudl, F. *J. Am. Chem. Soc.* **2008**, *130*, 6444.
(8) Yang, C.; Cho, S.; Heeger, A. J.; Wudl, F. *Angew. Chem., Int. Ed.* **2009**, *48*, 1592.
(9) Kooistra, F. B.; Mihailetchi, V. D.; Popescu, L. M.; Kronholm, D.; Blom, P. W. M.; Hummelen, J. C. *Chem. Mater.* **2006**, *18*, 3068.
(10) Anthony, J. E. *Angew. Chem., Int. Ed.* **2008**, *47*, 452.
(11) Takahashi, T.; Takenobu, T.; Takeya, J.; Iwasa, Y. *Appl. Phys. Lett.* **2006**, *88*, 3.
(12) Kowarik, S.; Gerlach, A.; Hinderhofer, A.; Milita, S.; Borgatti, F.; Zontone, F.; Suzuki, T.; Biscarini, F.; Schreiber, F. *Phys. Status Solidi RRL: Rapid Res. Lett.* **2008**, *2*, 120.
(13) Tang, M. L.; Reichardt, A. D.; Wei, P.; Bao, Z. N. *J. Am. Chem. Soc.* **2009**, *131*, 5264.
(14) Tang, M. L.; Reichardt, A. D.; Miyaki, N.; Stoltenberg, R. M.; Bao, Z. *J. Am. Chem. Soc.* **2008**, *130*, 6064.
(15) Swartz, C. R.; Parkin, S. R.; Bullock, J. E.; Anthony, J. E.; Mayer, A. C.; Malliaras, G. G. *Org. Lett.* **2005**, *7*, 3163.
(16) Ando, S.; Nishida, J.; Fujiwara, E.; Tada, H.; Inoue, Y.; Tokito, S.; Yamashita, Y. *Chem. Mater.* **2005**, *17*, 1261.
(17) Yamaguchi, S.; Tamao, K. *Bull. Chem. Soc. Jpn.* **1996**, *69*, 2327.
(18) Yamaguchi, S.; Tamao, K. *J. Chem. Soc., Dalton Trans.* **1998**, 3693.
(19) Yamaguchi, Y. *Synth. Met.* **1996**, *82*, 149.
(20) Ie, Y.; Nitani, M.; Karakawa, M.; Tada, H.; Aso, Y. *Adv. Funct. Mater.* **2010**, *20*, 907.
(21) Malenfant, P. R. L.; Dimitrakopoulos, C. D.; Gelorme, J. D.; Kosbar, L. L.; Graham, T. O.; Curioni, A.; Andreoni, W. *Appl. Phys. Lett.* **2002**, *80*, 2517.
(22) Chesterfield, R. J.; McKeen, J. C.; Newman, C. R.; Ewbank, P. C.; da Silva Filho, D. A.; Bredas, J.-L.; Miller, L. L.; Mann, K. R.; Frisbie, C. D. *J. Phys. Chem. B.* **2004**, *108*, 19281.
(23) Chen, F. C.; Liao, C. H. *Appl. Phys. Lett.* **2008**, *93*, 103310.
(24) Tatemichi, S.; Ichikawa, M.; Koyama, T.; Taniguchi, Y. *Appl. Phys. Lett.* **2006**, *89*, 112108.
(25) Oh, J. H.; Liu, S.; Bao, Z.; Schmidt, R.; Wurthner, F. *Appl. Phys. Lett.* **2007**, *91*, 212107.
(26) Jones, B. A.; Ahrens, M. J.; Yoon, M.-H.; Facchetti, A.; Marks, T. J.; Wasielewski, M. R. *Angew. Chem., Int. Ed.* **2004**, *43*, 6363.
(27) Molinari, A. S.; Alves, H.; Chen, Z.; Facchetti, A.; Morpurgo, A. F. *J. Am. Chem. Soc.* **2009**, *131*, 2462.
(28) Schmidt, R.; Oh, J. H.; Sun, Y. S.; Deppisch, M.; Krause, A. M.; Radacki, K.; Braunschweig, H.; Konemann, M.; Erk, P.; Bao, Z. A.; Wurthner, F. *J. Am. Chem. Soc.* **2009**, *131*, 6215.
(29) Katz, H. E.; Johnson, J.; Lovinger, A. J.; Li, W. J. *J. Am. Chem. Soc.* **2000**, *122*, 7787.
(30) Katz, H. E.; Lovinger, A. J.; Johnson, J.; Kloc, C.; Siegrist, T.; Li, W.; Lin, Y. Y.; Dodabalapur, A. *Nature* **2000**, *404*, 478.
(31) See, K. C.; Landis, C.; Sarjeant, A.; Katz, H. E. *Chem. Mater.* **2008**, *20*, 3609.
(32) (a) Jung, B. J.; Sun, J.; Lee, T.; Sarjeant, A.; Katz, H. E. *Chem. Mater.* **2009**, *21*, 94. (b) Shukla, D.; Nelson, S. F.; Freeman, D. C.; Rajeswaran, M.; Ahearn, W. G.; Meyer, D. M.; Carey, J. T. *Chem. Mater.* **2008**, *20*, 7486.

(33) Jones, B. A.; Facchetti, A.; Marks, T. J.; Wasielewski, M. R. *Chem. Mater.* **2007**, *19*, 2703.
(34) Zhan, X.; Facchetti, A.; Barlow, S.; Marks, T. J.; Ratner, M. A.; Wasielewski, M. R.; Marder, S. R. *Adv. Mater.* **2011**, *23*, 268.
(35) Anthony, J. E.; Facchetti, A.; Heeney, M.; Marder, S. R.; Zhan, X. *Adv. Mater.* **2010**, *22*, 3876.
(36) Zhan, X. W.; Tan, Z. A.; Domercq, B.; An, Z. S.; Zhang, X.; Barlow, S.; Li, Y. F.; Zhu, D. B.; Kippelen, B.; Marder, S. R. *J. Am. Chem. Soc.* **2007**, *129*, 7246.
(37) Zhan, X. W.; Tan, Z. A.; Zhou, E. J.; Li, Y. F.; Misra, R.; Grant, A.; Domercq, B.; Zhang, X. H.; An, Z. S.; Zhang, X.; Barlow, S.; Kippelen, B.; Marder, S. R. *J. Mater. Chem.* **2009**, *19*, 5794.
(38) Chen, Z. C.; Zheng, Y.; Yan, H.; Facchetti, A. *J. Am. Chem. Soc.* **2009**, *131*, 8.
(39) Huttner, S.; Sommer, M.; Thelakkat, M. *Appl. Phys. Lett.* **2008**, *92*, 093302.
(40) Guo, X. G.; Watson, M. D. *Org. Lett.* **2008**, *10*, 5333.
(41) Jones, B. A.; Facchetti, A.; Wasielewski, M. R.; Marks, T. J. *J. Am. Chem. Soc.* **2007**, *129*, 15259.
(42) Yan, H.; Chen, Z. H.; Zheng, Y.; Newman, C.; Quinn, J. R.; Dotz, F.; Kastler, M.; Facchetti, A. *Nature* **2009**, *457*, 679.
(43) Durban, M. M.; Kazarinoff, P. D.; Luscombe, C. K. *Macromolecules* **2010**, *43*, 6348.
(44) Kim, F. S.; Guo, X.; Watson, M. D.; Jenekhe, S. A. *Adv. Mater.* **2010**, *22*, 478.
(45) Szendrei, K.; Jarzab, D.; Chen, Z.; Facchetti, A.; Loi, M. A. *J. Mater. Chem.* **2010**, *20*, 1317.
(46) Usta, H.; Risko, C.; Wang, Z.; Huang, H.; Deliomeroglu, M. K.; Zhukhovitskiy, A.; Facchetti, A.; Marks, T. J. *J. Am. Chem. Soc.* **2009**, *131*, 5586.
(47) Freund, T.; Muellen, K.; Scherf, U. *Macromolecules* **1995**, *28*, 547.
(48) Overberger, C. G.; Moore, J. A. *Adv. Polym. Sci.* **1970**, *7*, 113.
(49) Schlueter, A. D. *Adv. Mater.* **1991**, *3*, 282.
(50) Yu, L.; Chen, M.; Dalton, L. R. *Chem. Mater.* **1990**, *2*, 649.
(51) Hong, S. Y.; Kertesz, M.; Lee, Y. S.; Kim, O.-K. *Chem. Mater.* **1992**, *4*, 378.
(52) Godt, A.; Schlüter, A.-D. *Adv. Mater.* **1991**, *3*, 497.
(53) Yu., L.; Dalton, L. R. *Macromolecules* **1990**, *23*, 3439.
(54) Scherf, U.; Müllen, K. *Synthesis* **1992**, 23.
(55) Schlüter, A.-D.; Schlicke, B. *Synlett.* **1996**, 425.
(56) Kertesz, M.; Hong, S. Y. *Macromolecules* **1992**, *25*, 5424.
(57) Kintzel, O.; Münch, W.; Schlüter, A.-D.; Godt, A. *J. Org. Chem.* **1996**, *61*, 7304.
(58) Scherf, U.; Müllen, K. *Adv. Polym. Sci.* **1995**, *123*, 1.
(59) Roncali, J. *Chem. Rev.* **1997**, 1733.
(60) Dai, Y.; Katz, T. J.; Nichols, D. A. *Angew. Chem., Int. Ed. Engl.* **1996**, *35*, 2109.
(61) Goldfinger, M. B.; Swager, T. M. *J. Am. Chem. Soc.* **1994**, *116*, 7895.
(62) Briseno, A.; Mannsfeld, S. C. B.; Shamberger, P. J.; Ohuchi, F. S.; Bao, Z.; Jenekhe, S. A.; Xia, Y. *Chem. Mater.* **2008**, *20*, 4712.
(63) Chen, Y.; Huang, W.; Li, C.; Bo, Z. *Macromolecules* **2010**, *43*, 10216.
(64) Zhang, Q. T.; Tour, J. M. *J. Am. Chem. Soc.* **1997**, *119*, 9624.
(65) Yao, Y.; Lamba, J. J. S.; Tour, J. M. *J. Am. Chem. Soc.* **1998**, *120*, 2805.
(66) Yao, Y.; Zhang, Q. T.; Tour, J. M. *Macromolecules* **1998**, *31*, 8600.
(67) Lamba, J. J. S.; Tour, J. M. *J. Am. Chem. Soc.* **1994**, *116*, 11723.
(68) Becke, A. D. *J. Chem. Phys.* **1993**, *98*, 5648.
(69) Lee, C.; Yang, W.; Parr, R. G. *Phys. Rev. B* **1988**, *37*, 785.
(70) Frisch, M. J. et al. *Gaussian 03*, revision E.01; Gaussian, Inc.: Pittsburgh, PA, 2003.
(71) Chen, Z.; Zheng, Y.; Yan, H.; Facchetti, A. *J. Am. Chem. Soc.* **2009**, *131*, 8.
(72) Koeckelberghs, G.; De Cremer, L.; Vanormelingen, W.; Dehaen, W.; Verbiest, T.; Persoons, A.; Samyn, C. *Tetrahedron* **2005**, *61*, 687.
(73) Kaim, W.; Tesmann, H.; Bock, H. *Chem. Ber* **1980**, *113*, 3221.
(74) Yao, Y.; Tour, J. M. *Macromolecules* **1999**, *32*, 2455.
(75) Avila-Ortega, A.; Vazquez-Torres, H. *J. Polym. Sci. A1* **2007**, *45*, 1993.
(76) Li, Y. F.; Cao, Y.; Gao, J.; Wang, D. L.; Yu, G.; Heeger, A. J. *Synth. Met.* **1999**, *99*, 243.
(77) Singh, T. B.; Erten, S.; Guenes, S.; Zafer, C.; Turkmen, G.; Kuban, B.; Teoman, Y.; Sariciftci, N. S.; Icli, S. *Org. Electron.* **2006**, *7*, 480.
(78) Kang, S.-M.; Leblebici, Y. *CMOS Digital Integrated Circuits: Analysis and Design*; McGraw-Hill: NewYork, 1996.